Three-axle vehicle lateral dynamics identification using double lane change maneuvers data*

Camila L. Pereira[1], Daniel H. B. de Sousa[1] and Helon V. H. Ayala[1]

Abstract— The study of lateral dynamics is of great importance for the vehicle behavior analysis during turning maneuvers, and it is fundamental to stability or path control systems used in autonomous vehicles. This case study focuses on the identification of a continuous-time linear model of a 6x6 military vehicle for different speeds. Field data of the vehicle during a North Atlantic Treaty Organization (NATO) double lane change maneuvers were used, and transfer functions between the yaw rate (output) and the steering wheel angle (input) were identified using the CONTSID toolbox. Based on the estimated models, the results show a good agreement with the experimental measurements and it is possible to analyze the system's poles and zeros behavior, as well as the frequency response of the system with speed variation. As conclusions, an increase in the vehicle's speed implies a higher magnitude gain, and the poles of the system present the tendency to move from an underdamped to an overdamped system.

I. INTRODUCTION

Models and simulations are essential for vehicles' development and improvement since they allow, for instance, performance prediction, parameter adjustments, and advances in integrated control systems. There are several approaches in the literature to model a vehicle dynamics behavior, chosen usually based on its complexity; the specific motion evaluated; and the available information, such as experimental measurements, which may lead to a data-based approach for model estimation. Regarding the latter, the estimation of parameters, states, and models using system identification methods is a relevant alternative, especially due to under-modeling and parameter uncertainties that may affect the mathematical formulation [1].

Lateral dynamics analysis is of great importance to predict the vehicle's behavior during steering maneuvers. This knowledge allows the project of more efficient and precise stability and path control systems, which are essential not only for vehicle safety improvement but also for autonomous vehicle development. In the military field, the application of a stabilization control system assists the driver in the maneuvering of the vehicle, especially Armored Personnel Carrier (APC) vehicles due to their size and weight [2], [3]. In this context, one of the main applications of dynamic models is in the synthesis of the vehicle's control systems. A review of the most used models and control strategies for path control systems is presented in [4], being the well-known two degrees-of-freedom (DOF) bicycle model (single-track model) the most commonly applied [5].

In [6] a modified Denavit-Hartenberg convention is used with Newton-Euler equations to derive a multi-body dynamic model of the vehicle. The model was validated using SCANeR-studio™ simulator and presented good results for a large marge of driving conditions. Even though multibodies models are more representative of a system's dynamics when compared to classical closed-form models, it is more complex, since the number of DOF is usually higher and a better knowledge of the system topology to describe the connections between each body is needed.

One of the strategies to obtain a model is through system identification and for this purpose several toolboxes were developed, including MATLAB® System Identification and the CONtinuous-Time System IDentification (CONTSID) toolboxes. According to [7], CONTSID provides MATLAB® functions to estimate linear system mathematical models, such as transfer functions and state-space models, using input/output measurements of the dynamical system through parameters' identification. This toolbox has already been used in [8] for estimation of a second-order system to simulate drivability relevant vibrations in passenger cars.

Regarding the identification of models for a dynamic system, [1] applies three subspace identification methods for vehicle lateral dynamics modeling using the input/output data: Multivariable Output Error State Space (MOESP), Numerical Algorithms for Subspace State Space System Identification (N4SID), and Canonical Variate Analysis (CVA). The model structure is based on a single-track model with two DOF; and a pulse input, a step input, and a double lane change test maneuvers at a constant vehicle speed were carried out for data acquisition. Results show that the proposed data-driven modeling approaches present a good agreement with the measured data. However, experiments were conducted for a single speed value.

An estimator based on an Extended Kalman-Filter (EKF) and the bicycle model is used in [9] to identify the vehicle's states and the cornering stiffness of the tires. A similar methodology is applied in [10] to identify the model's states and changes in the vehicle mass. Although the simulation results show that the proposed approach outperforms the standard implementation with constant mass, the EFK observer may have poor performance under low excitation conditions. In order to estimate tire side-slip angle and lateral forces, [11] combines an adaptive-sliding-mode observer with an adaptive compensation algorithm, using the bicycle model and a four-wheel three DOF vehicle model. Nevertheless, uncertainties in vehicle parameters and noise in the measurements could affect the estimator performance.

A three DOF four-wheel vehicle model is used in [12] to estimate the longitudinal force, lateral speed, and yaw rate, combining a longitudinal force observer and a tracking filter algorithm, demanding extensive mathematical development.

Ref. [13] applies an Artificial Neural Network (ANN) to estimate the side-slip angle during maneuvers at different speeds using CarSim™. However, it is focused on the estimation of a single parameter model, and a comparison with field measurements is not presented. As can be noted, most of the papers are based on modeling a common four-wheel single-steering axle vehicle, which poses a lack of research on vehicles with more than two and multiple-steering axles.

In this context, this work aims to present a case study regarding the identification of a continuous-time linear model of a 6x6 APC military vehicle using the CONTSID toolbox and data of the test vehicle during a double lane change maneuver. The model structure selection and parameters estimation were based on system identification methods implemented in this toolbox and the single-track model formulation for a three-axle vehicle. The estimated transfer function between the yaw rate (output) and the wheel steering angle (input) for different speeds is evaluated, and the influence of the velocity on the frequency response and the poles and zeros behavior is analyzed. These models give an insight into the lateral dynamics response and configure the first step to further research regarding stability and path control. Therefore, the main contributions of this paper are the application of data-driven identification techniques to estimate continuous-time models for a 6x6 military vehicle lateral dynamics, and an analysis of the influence of speed on the estimated models response.

The paper is structured as follows. Section II presents the proposed case study, while Section III addresses the mathematical formulation of a single-track model of the vehicle as an approach for a model structure definition. The methodology for the continuous-time linear model identification is developed in Section IV. The resultant models and the effects of the speed variation are discussed in Section V. Conclusive remarks are drawn in Section VI.

II. CASE STUDY

The identification problem case study consists of using experimental data acquired during double lane change maneuvers of a 6x6 military vehicle at different speeds to select a model structure; estimate the parameters of the transfer functions between the yaw rate (output) and the wheel steering angle (input) for different velocities, and; compare the resultant model to the field data for acceptance.

A. Experiment description

The experimental measurements used are from a three-axle APC military vehicle with the front and middle axles steerable. The data were acquired during double lane change maneuvers performed according to the North Atlantic Treaty Organization (NATO) Allied Vehicle Testing Publications (AVTP) 03-160W standard [14]. This test is usually considered to assess the lateral stability of a vehicle, and it is also one of the most used for state and parameters identification related to lateral dynamics. The maneuver consists of the transition from a right lane to a left lane, and then return to the initial right lane afterward. A test track was set up according to the layout provided in [14], based on the vehicle dimensions given in Table I. The vehicle selected for data acquisition is presented in Fig. 1.

TABLE I

VEHICLE'S INFORMATION

Parameter	Symbol	Value
Mass	m	15,770 kg
Length	L	7.10 m
Height	H	2.60 m
Width	w_v	3.30 m
Distance from CG to front axle	a_1	1.77 m
Distance from CG to middle axle	a_2	0.07 m
Distance from CG to rear axle	a_3	1.93 m

Fig. 1. Vehicle used for experimental measurements

Measurement data were collected using the following equipment: a data logger VBOX 3i from Racelogic®; an inertial measurement unit (IMU) model RLVBIMU04 from Racelogic® fixed on the floor of the troop compartment for pitch, roll, and yaw rates, as well as x, y, z acceleration; a global positioning system (GPS) antenna positioned on the external top of the vehicle for velocity and traveled distance acquisition; and a draw-wire displacement sensor from MICRO-EPSILON® mounted in the auxiliary steering cylinder of the front left wheel to obtain the wheel steering angle using an experimental linear relation between the transducer's displacement and the wheel steering angle.

An unladen vehicle performed double lane change maneuvers at 10 km/h, 20 km/h, 30 km/h, 40 km/h, 50 km/h, 60 km/h, 70 km/h and 80 km/h. Data were recorded at 100 Hz and saved for subsequent analysis. An example of the measurements acquired is presented in Fig. 2. The yaw rate and the wheel steering angle are the variables of interest in this study given that the measured output values of the yaw rate are more reliable in comparison to the lateral acceleration, while the wheel steering angle was selected as the input of the transfer function model.

Data preprocessing on the measured data is crucial to compensate disturbances caused mainly by the vibration resultant of the running engine and sensors' offset. Therefore, a 12-order Butterworth filter with a normalized cutoff frequency of 2.5 Hz-3.5 Hz was applied to the yaw rate and steering wheel angle based on those signals' spectrograms. This filter removed high-frequency content from other sources, such as noise and vehicle vibration. Also, zero-phase digital filtering was applied to remove the phase delay of the filtered signal. The sensor offset had to be compensated since it was significant in the measurements of the wheel steering angle and the lateral acceleration, as can be seen in Fig. 2. It is important to highlight that the driver was responsible to maintain the

vehicle's speed during each maneuver. Consequently, besides the data filtering, trends and outliers were removed to select useful portions of the original data.
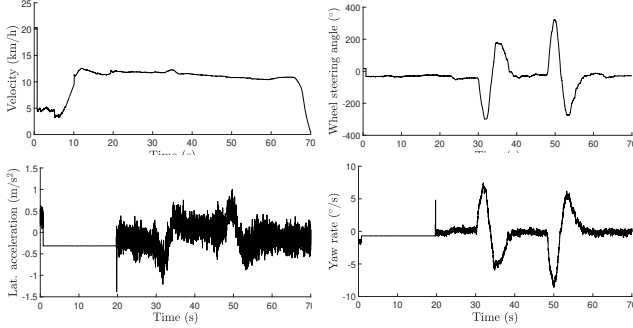

Fig. 2. Raw data of the vehicle during a double lane change maneuver performed at, approximately, 10 km/h

Another aspect that can be evaluated is the frequency domain spectrum of the wheel steering angle and the yaw rate since it allows the evaluation of the measurements over a range of frequencies. According to Fig. 3 and Fig. 4, it is possible to conclude that the signals are concentrated in low frequencies, which is significant for the estimated models application.
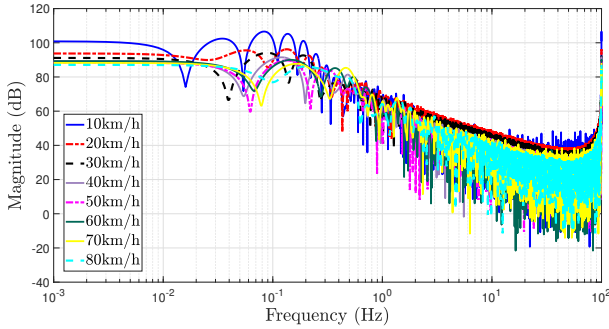

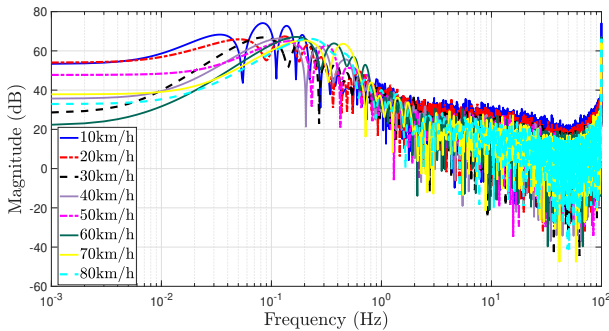Fig. 3. Wheel steering angle spectrum in the frequency domain

Fig. 4. Yaw rate spectrum in the frequency domain

III. VEHICLE MODEL

The mathematical formulation based on a physical model is one of the main approaches to represent a dynamic system. In order to define a linear structure, the single-track model was considered to represent the lateral dynamics, writing the linearized Newton-Euler equation of motion on the xy plane of the forces acting on each axle, assuming that both wheels per axle are expressed by a single equivalent wheel. Fig. 5 shows a schematic representation of the model, where v is

the velocity vector of the vehicle, r is the yaw rate, while δ_f and δ_m are the front and middle steering angles of the front ad middle wheel.
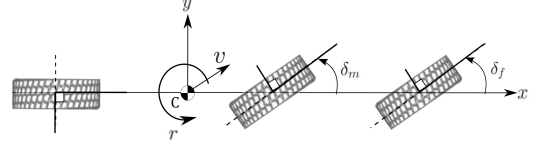

Fig. 5. Single-track model of a three-axle vehicle

For small steer angles and under the linear handling regime of the tires, the lateral forces F_y acting on the tires can be considered as a linear function of the slip angle α, such that $F_y = -C_\alpha \alpha$, where C_α is the tire's cornering stiffness [15]. Based on the linearized single-track model for a two-axle vehicle presented in [15], assuming a constant forward speed and no roll motion, an analogous two DOF model for a three-axle vehicle was obtained as a function of the lateral velocity, v_y, the yaw rate r, the vehicle mass m, the tires' cornering stiffness, the axles' distances to the vehicle's CG, the moment of inertia I_z and the equivalent steer angle δ_f

$$\begin{bmatrix} \dot{v}_y \\ \dot{r} \end{bmatrix} = A \begin{bmatrix} v_y \\ r \end{bmatrix} + B\delta_f, \tag{1}$$

where:

$$A = \begin{bmatrix} A_{11} & A_{12} \\ A_{21} & A_{22} \end{bmatrix} =$$

$$\begin{bmatrix} -\dfrac{C_{\alpha_f}+C_{\alpha_m}+C_{\alpha_r}}{mv_x} & \dfrac{-a_1 C_{\alpha_f}-a_2 C_{\alpha_m}+a_3 C_{\alpha_r}}{mv_x} - v_x \\ -\dfrac{a_1 C_{\alpha_f}+a_2 C_{\alpha_m}-a_3 C_{\alpha_r}}{I_z v_x} & -\dfrac{a_1^2 C_{\alpha_f}+a_2^2 C_{\alpha_m}+a_3^2 C_{\alpha_r}}{I_z v_x} \end{bmatrix}, \tag{2}$$

$$B = \begin{bmatrix} B_1 \\ B_2 \end{bmatrix} = \begin{bmatrix} \dfrac{C_{\alpha_f}}{m} + \left(\dfrac{a_2+a_3}{a_1+a_3}\right)\dfrac{C_{\alpha_m}}{m} \\ \dfrac{a_1 C_{\alpha_f}}{I_z} + \left(\dfrac{a_2+a_3}{a_1+a_3}\right)\dfrac{a_2 C_{\alpha_m}}{I_z} \end{bmatrix}, \tag{3}$$

considering a linear relation between the middle and front wheel steer angles obtained using the Ackermann geometry:

$$\delta_m = \tan^{-1}\left(\dfrac{a_3+a_2}{a_3+a_1}\tan(\delta_f)\right) \approx \dfrac{a_2+a_3}{a_1+a_3}\delta_f. \tag{4}$$

Therefore, from the Laplace domain equations of motion expressed by (1), the structure of the transfer function $G_\delta^r(s)$ for the yaw rate, considering the steering angle of the front wheel as the input, presents two poles and one zero, which vary with the elements of the matrix A and the vector B, given by:

$$\begin{aligned} G_\delta^r(s) &= \dfrac{r(s)}{\delta_f(s)} \\ &= \dfrac{(A_{21}B_1 B_2)s - (A_{11}A_{21}B_1 B_2)}{s^2 - (A_{11}+A_{22})s + (A_{22}A_{11}-A_{12}A_{21})}. \end{aligned} \tag{5}$$

Assuming that there is a linear relationship between the front wheel steer angle and the wheel steering angle, such as a steering ratio, this structure is still valid for a transfer function considering the wheel steering angle as the input.

912

IV. CONTINUOUS-TIME SYSTEM IDENTIFICATION APPLIED TO LATERAL DYNAMICS MODELING

In this section, we give the details of the identification procedure adopted to estimate linear models of the lateral dynamics for different speeds using experimental data of the vehicle obtained according to Sec. II.

A. Algorithmic Procedure

In order to estimate a continuous-time transfer function model between the sampled data of the yaw rate and the wheel steering angle, a system identification procedure using the CONTSID toolbox was applied. The process consisted of the following steps based on the recommended sequence workflow for system identification presented in [7]:

1) acquisition of the time-domain input/output data from the double lane change maneuvers;
2) selection and preprocessing of useful portions of the data for each speed. This step includes the spectrogram analysis of the input/output signals, noise reduction with filtering and offset removal;
3) definition and selection of a model structure (a set of candidate system descriptions) ;
4) estimation of the transfer function parameters of the model structure using post-processing input/output data, the selected model structure, and the CONTSID toolbox; and
5) evaluation of the estimated model fit to the experimental data based on the multiple correlation coefficient R^2 between the estimated model response $\hat{y}$ and the measurements $y(t)$. As a guideline, $R^2 > 0.9$ is considered satisfactory for many applications [16].

B. Identification problem formulation

A description of steps 1 and 2 of the previous algorithm procedure was already presented in Sec. II-A. Regarding the definition of the model structure (step 3), two approaches were used. The first was the linear transfer function between the yaw rate and steering wheel angle obtained through the single-track model, explained in Sec. III. The second was a model order selection function based on the Refined Instrumental Variable for Continuous-time (RIVC) method, available in CONTSID, to automatically search over a whole range of different model orders, providing a set of best structures according to the Young Information Criterion (YIC) and the associated coefficient of determination R_T^2 criteria. The selection of the final model structure was based on the common set of values for different speeds.

As for the approach using the CONTSID toolbox, it was considered the range of one to two numerator parameters and two to five denominator parameters as inputs for the model selection function. Then, the method returned the selected model structures for each set of input/output measured data for each speed. The common structures for all the speeds evaluated were two poles and a zero, in agreement with the first approach in Sec. III; and three poles and a zero. Consequently, both structures candidates were analyzed to verify the influence of the vehicle's speed on the yaw rate

frequency response and the poles and zeros behavior of the system. Given the post-processed input/output measurements and the selected structure of the transfer function (number of poles and zeros), the CONTSID toolbox was applied to estimate the parameters of continuous-time output-error models using the Simple Refined Instrumental Variable (IV) for Continuous-time models (SRIVC) estimation method.

V. RESULTS AND DISCUSSION

Following the methodology presented in Sec. IV and using the double lane change test data for different velocities, transfer functions considering the yaw rate as the output and the wheel steering angle as the input were estimated. Thus, the influence of the speed on the identified models can be verified, such as its frequency response and the poles and zeros behavior.

The estimated poles and zeros of the transfer functions and the respective R^2 coefficients are presented in Table II, while Fig. 6 exhibits the comparison between raw data, filtered measurements, and the model's response for each velocity. It can be noticed that the resultant models satisfactorily match the measured data, with $R^2 > 0.94$. Since both wheel steering angle and yaw rate measurements are concentrated in low frequencies, the estimated models are valid for this range.

TABLE II
ESTIMATED MODEL'S PARAMETERS FOR DIFFERENT VELOCITIES

Velocity	Poles	Zeros	R^2
10 km/h	$-2.3265 + 7.4728i$ $-2.3265 - 7.4728i$	11.3127	0.9917
20 km/h	$-5.1831 + 6.8630i$ $-5.1831 - 6.8630i$	11.1322	0.9884
30 km/h	-3.1019 -0.3773	-0.3218	0.9823
40 km/h	$-9.3074 + 3.2495i$ $-9.3074 - 3.2495i$	11.0330	0.9910
50 km/h	$-6.8074 + 3.7529i$ $-6.8074 - 3.7529i$	15.7413	0.9915
60 km/h	-2.9798 -0.0799	0.0877	0.9426
70 km/h	$-4.2729 + 3.6978i$ $-4.2729 - 3.6978i$	24.5142	0.9825
80 km/h	-11.2494 -3.8269	16.9710	0.9820

Besides that, the frequency response analysis may provide information regarding the vehicle's performance during a maneuver. The influence of the speed on the frequency response of the second-order model structure can be examined in the Bode plot in Fig. 7. It is verified that an increase in the speed implies a positive increase in the steady-state magnitude and the phase lag after 1 Hz, in agreement with the conclusions of the theoretical studies presented in [17] and [18]. One important characteristic to be evaluated is the yaw rate response gain related to its static value since minimum increments are desirable for better handling and stability [19]. From the magnitude plot in Fig. 7, the highest peaks correspond to the lowest velocities.
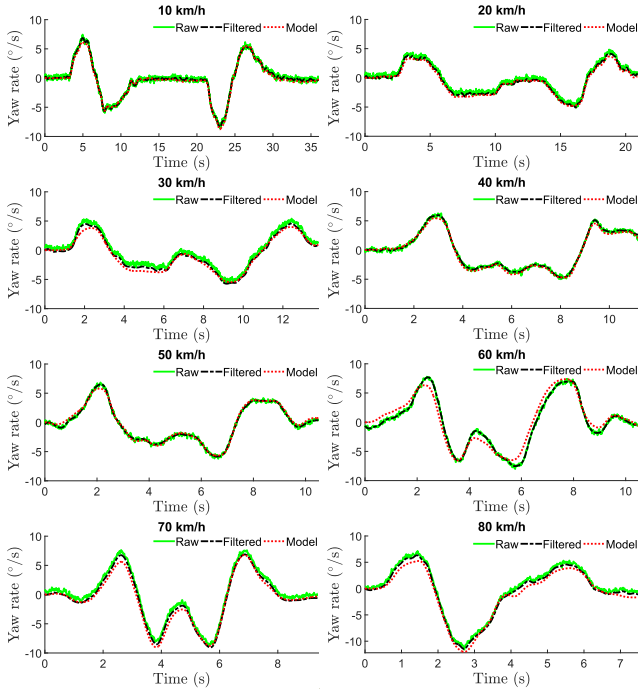
Fig. 6.   Raw, filtered and estimated model's yaw rate response

Fig. 7.   Bode plots of the magnitude and phase change of the yaw rate with respect to the speed variation of the vehicle

According to the analysis presented in [18], it is possible to observe that the vehicle changes its handling characteristic from understeer, at lower speeds, to a neutral steer behavior at higher speeds, which may affect the vehicle's lateral stability. An understeer tendency implies that the steering angles are higher with increasing speed to keep the same curve radius, while the opposite is true for the oversteer conditions. For a neutral steer vehicle, the same steering angle is maintained to keep the same turning circle. It is important to highlight that an understeer behavior is considered stable, while oversteer is unstable since it is more difficult for the driver to regain control over the vehicle.

From Fig. 7, it is also possible to notice that at low frequencies (lower than 0.1 Hz), the phase graphic has an initial phase lag of approximately $180°$ (input-output out of phase), which diverges from the value of $0°$ predicted in the analysis done in [18]. This divergence was caused by the phase lag on the measurement data of steering angle and yaw rate. At intermediate frequencies, between 0.1 Hz and 1 Hz, there is a growing negative phase lag, while for higher frequencies, the phase for most velocity values tends to converge to $-80°$. The exceptions are the models for 30 km/h and 60 km/h, which were the only ones with a negative zero, whose phases tend to $100°$.

The influence of the speed variation on the poles and zeros behavior can be visualized in Fig. 8. The poles are located at the left half of the s-plane (negative real components), which is an indication of the system's stability. Additionally, they tend to move from an underdamped system (imaginary poles) at lower speeds to an overdamped system (real poles) at higher speeds. According to the obtained models, most of the zeros are located in the right half of the s-plane, i.e.,
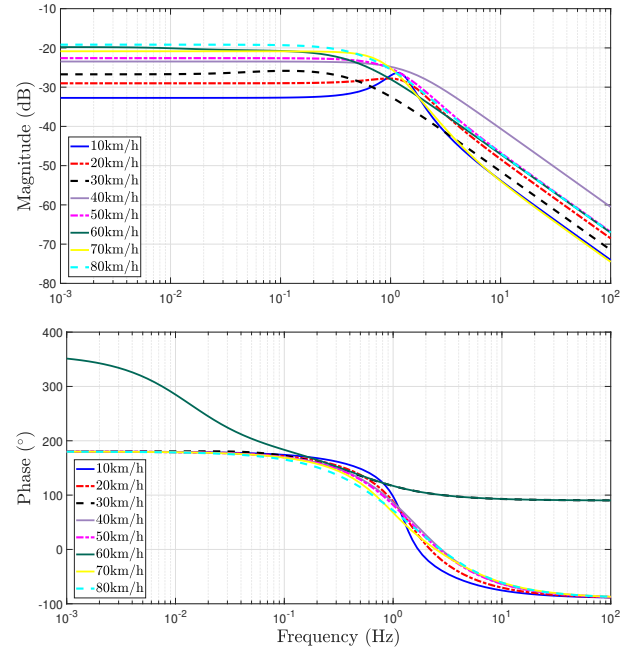
non-minimum phase zeros, which implies that the system has non-minimum phase characteristics. According to [20], this can cause the response to initially start in the opposite direction.
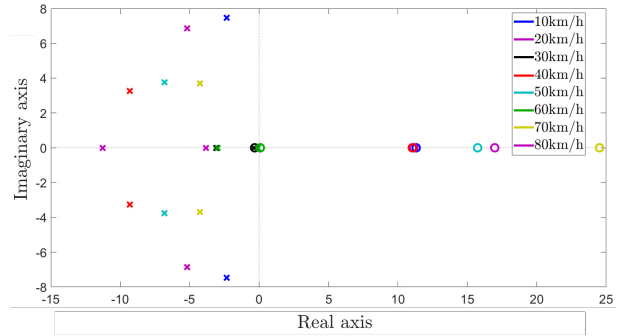

Fig. 8.   Poles and zeros behavior with vehicle's speed variation

The same procedure applied to the third-order model structure resulted in poles canceling zeros for most velocities, which could imply that some of the parameters added are not relevant, i.e., with the increase in the complexity of the model structure, the identification algorithm cancels the influence of additional poles with zeros to obtain the best fitting response. According to [7], higher-order models are not always more accurate and they also contribute to increase the uncertainties of the parameters. It is highlighted, though, that significant variations in the estimated CONTSID models were verified with modifications on the data preprocessing process, particularly regarding the offset removal and window selection.

Another issue is that, as already mentioned, the input-output data is concentrated at low frequencies. Therefore, the identified models are considered representations of the system in that range. In order to obtain a model that completely

describes the system, more information is required. For instance, [13] applied a swept sine type signal in simulations to generate enough data of a system to train an ANN. For the case study in focus, the data are acquired during double lane change maneuvers performed following NATO AVTP 03-160W standard, and due to the vehicle's dimensions and safety measures, it is not possible to generate input-output signals of higher frequencies, bearing in mind that the input is the steering wheel angle and the output is the yaw rate.

VI. CONCLUSIONS

This work presented a case study regarding a 6x6 military vehicle using the CONTSID toolbox for the identification of a continuous-time linear model of the lateral dynamics using measurements of the vehicle during NATO double lane change maneuvers performed at different speeds. This approach relies on the input-output measured data and it does not require knowledge of the vehicle's parameters, which could be unknown and difficult to measure. The transfer function parameters between the wheel steering angle (input) and the yaw rate (output) were estimated through the Simple Refined Instrumental Variable for Continuous-time models estimation method implemented in CONTSID.

According to the results, the estimated models presented a good agreement with the experimental data. Given the frequency response of the identified models, it was concluded that an increase in the vehicle's speed implies a higher magnitude gain, and the poles of the system present the tendency to move from an underdamped system (imaginary poles) at lower speeds to an overdamped system (real poles) at higher speeds. Based on the input/output signals, it is possible to conclude that they are concentrated at low frequencies, where the obtained models would be valid. Further research will focus on the following aspects:

- closed-loop system identification to improve the spectrums of the input-output signals and the estimated models, using experiment design such as in [21];
- identifiability of physical parameters in the frequency domain, as performed in [22];
- adaptive identifiability for friction properties and cornering stiffness estimation, similar to the study developed in [23]; and
- model predictive control (MPC) and adaptive identifiability for path-following purpose, which are relevant for complex environments, as can be seen in [24].

REFERENCES

[1] T. Ba, X. Guan, and J. Zhang, "Vehicle lateral dynamics modelling by subspace identification methods and tyre cornering stiffness estimation," *International Journal of Vehicle Systems Modelling and Testing*, vol. 10, no. 4, pp. 340–355, 2015.

[2] E. Quintana, "The ethics and legal implications of military unmanned vehicles," *RUSI, Occasional Paper*, 2008.

[3] J. M. Anderson, B. Arbour, R. Arnold, T. Kadiofsky, T. Keeley, M. R. MacLeod, S. Bourdon, R. Crootof, J. Matsumura, C. Mayer, *et al.*, "Autonomous systems: Issues for defence policymakers," NATO Allied Command Transformation, Tech. Rep., 2015.

[4] N. H. Amer, H. Zamzuri, K. Hudha, and Z. A. Kadir, "Modelling and control strategies in path tracking control for autonomous ground vehicles: a review of state of the art and challenges," *Journal of intelligent & robotic systems*, vol. 86, no. 2, pp. 225–254, 2017.

[5] B. Arifin, B. Y. Suprapto, S. A. D. Prasetyowati, and Z. Nawawi, "The lateral control of autonomous vehicles: A review," in *2019 International Conference on Electrical Engineering and Computer Science (ICECOS)*. IEEE, 2019, pp. 277–282.

[6] A. Chebly, R. Talj, and A. Charara, "Coupled longitudinal and lateral control for an autonomous vehicle dynamics modeled using a robotics formalism," *IFAC-PapersOnLine*, vol. 50, no. 1, pp. 12526–12532, 2017.

[7] H. Garnier and M. Gilson, "CONTSID: a matlab toolbox for standard and advanced identification of black-box continuous-time models," *IFAC-PapersOnLine*, vol. 51, no. 15, pp. 688–693, 2018.

[8] K. J. Figel, M. Schultalbers, and F. Svaricek, "Experimental analysis of driveline shuffle with focus on the interaction between traction and torsional vibrations," *IFAC-PapersOnLine*, vol. 52, no. 5, pp. 322–328, 2019.

[9] G. Reina and A. Messina, "Vehicle dynamics estimation via augmented Extended Kalman Filtering," *Measurement*, vol. 133, pp. 383–395, 2019.

[10] G. Reina, M. Paiano, and J.-L. Blanco-Claraco, "Vehicle parameter estimation using a model-based estimator," *Mechanical Systems and Signal Processing*, vol. 87, pp. 227–241, 2017.

[11] S. Cheng, L. Li, B. Yan, C. Liu, X. Wang, and J. Fang, "Simultaneous estimation of tire side-slip angle and lateral tire force for vehicle lateral stability control," *Mechanical Systems and Signal Processing*, vol. 132, pp. 168–182, 2019.

[12] T. Chen, X. Xu, L. Chen, H. Jiang, Y. Cai, and Y. Li, "Estimation of longitudinal force, lateral vehicle speed and yaw rate for four-wheel independent driven electric vehicles," *Mechanical Systems and Signal Processing*, vol. 101, pp. 377–388, 2018.

[13] D. Chindamo and M. Gadola, "Estimation of vehicle side-slip angle using an artificial neural network," in *MATEC web of conferences*, vol. 166. EDP Sciences, 2018, p. 02001.

[14] North Atlantic Treaty Organization (NATO), "NATO Dynamic Stability, Allied Vehicle Testing Publications (AVTP) 03-160 W," pp. 665–725, 1991.

[15] N. Jazar, *Vehicle Dynamics, Theory and Application*. Riverdale, NY: Springer, 2008.

[16] B. Schaible, H. Xie, and Y.-C. Lee, "Fuzzy logic models for ranking process effects," *IEEE Transactions on Fuzzy Systems*, vol. 5, no. 4, pp. 545–556, 1997.

[17] J.-H. Jang and C.-S. Han, "The sensitivity analysis of yaw rate for a front wheel steering vehicle: In the frequency domain," *KSME International Journal*, vol. 11, no. 1, pp. 56–66, 1997.

[18] M. Abe, *Vehicle handling dynamics: theory and application*. Butterworth-Heinemann, 2015.

[19] T. J. Yuen, S. M. Foong, and R. Ramli, "Optimized suspension kinematic profiles for handling performance using 10-degree-of-freedom vehicle model," *Proceedings of the Institution of Mechanical Engineers, Part K: Journal of Multi-body Dynamics*, vol. 228, no. 1, pp. 82–99, 2014.

[20] J. Kiefer, "Modeling of road vehicle lateral dynamics," Master's thesis, Rochester Institute of Technology, 1996.

[21] P. Shah and R. Sekhar, "Closed loop system identification of a dc motor using fractional order model," in *2019 International Conference on Mechatronics, Robotics and Systems Engineering (MoRSE)*. IEEE, 2019, pp. 69–74.

[22] E. Popp, M. Tantau, M. Wielitzka, T. Ortmaier, and D. Giebert, "Frequency domain identification and identifiability analysis of a nonlinear vehicle drivetrain model," in *2019 18th European Control Conference (ECC)*. IEEE, 2019, pp. 237–242.

[23] A. Lopes and R. E. Araújo, "Vehicle lateral dynamic identification method based on adaptive algorithm," *IEEE Open Journal of Vehicular Technology*, vol. 1, pp. 267–278, 2020.

[24] F. Lin, Y. Chen, Y. Zhao, and S. Wang, "Path tracking of autonomous vehicle based on adaptive model predictive control," *International Journal of Advanced Robotic Systems*, vol. 16, no. 5, p. 1729881419880089, 2019.